1521-0111/101/6/400–407$35.00
MOLECULAR PHARMACOLOGY

dx.doi.org/10.1124/molpharm.122.000502
Mol Pharmacol 101:400–407, June 2022

Secretin Amino-Terminal Structure-Activity Relationships and Complementary Mutagenesis at the Site of Docking to the Secretin Receptor

Juliana E. Milburn, Kaleeckal G. Harikumar, Sarah J. Piper, Sweta Raval, Arthur Christopoulos, Denise Wootten, Patrick M. Sexton, and Laurence J. Miller

Department of Molecular Pharmacology and Experimental Therapeutics, Mayo Clinic, Scottsdale, Arizona (J.E.M., K.G.H., S.R., L.J.M.) and Drug Discovery Biology and Australian Research Council Centre for Cryo-Electron Microscopy of Membrane Proteins, Monash Institute of Pharmaceutical Sciences, Monash University, Parkville, Australia (S.J.P., A.C., D.W., P.M.S.)

Received February 9, 2022; accepted March 22, 2022

ABSTRACT

Class B1 G protein–coupled receptors are activated by peptides, with amino-terminal regions critical for biologic activity. Although high resolution structures exist, understanding of key features of the peptide activation domain that drive signaling is limited. In the secretin receptor (SecR) structure, interactions are observed between peptide residues His^1 and Ser^2 and seventh transmembrane segment (TM7) receptor residue E373. We interrogated these interactions using systematic structure-activity analysis of peptide and receptor. His^1 was critical for binding and cAMP responses, but its orientation was not critical, and substitution could independently modify affinity and efficacy. Ser^2 was also critical, with all substitutions reducing peptide affinity and functional responses proportionally. Mutation of E373 to conserved acidic Asp (E373D), uncharged polar Gln (E373Q), or charge-reversed basic Arg (E373R) did not alter receptor expression, with all exhibiting secretin-dependent cAMP accumulation. All position 373 mutants displayed reduced binding affinities and cAMP potencies for many peptide analogs, although relative effects of position 1 peptides were similar whereas position 2 peptides exhibited substantial differences. The peptide including basic Lys in position 2 was active at SecR having acidic Glu in position 373 and at E373D while exhibiting minimal activity at those receptors in which an acidic residue is absent in this position (E373Q and E373R). In contrast, the peptide including acidic Glu in position 2 was equipotent with secretin at E373R while being much less potent than secretin at wild-type SecR and E373D. These data support functional importance of a charge-charge interaction between the amino-terminal region of secretin and the top of TM7.

SIGNIFICANCE STATEMENT

This work refines our molecular understanding of the activation mechanisms of class B1 G protein–coupled receptors. The amino-terminal region of secretin interacts with the seventh transmembrane segment of its receptor with structural specificity and with a charge-charge interaction helping to drive functional activation.

Introduction

Class B1 G protein–coupled receptors (GPCRs) bind and become activated by moderate length peptide ligands that use a two-step process in their docking (Hoare, 2005). The carboxyl terminus (C terminus) of the peptide first docks within a groove in the disulfide-bonded receptor amino-terminal (N-terminal) extracellular domain (ECD), and then the peptide amino terminus (N terminus) is oriented toward the upper region of the transmembrane helical bundle (junctional domain) (Castro et al., 2005; Parthier et al., 2009). The first step is a major contributor to the peptide binding affinity, whereas the second step is required for receptor activation and functional responses (Miller et al., 2012; Watkins et al., 2012). The molecular determinants of peptide interaction with the ECD are generally well understood, with insight initially from carboxyl-terminal (C-terminal) peptide-bound ECD structures (Grace et al., 2004, 2007) and more recently from peptide-occupied holoreceptor structures (Hollenstein et al., 2014; de Graaf et al., 2016, 2017; Schwartz and Frimurer, 2017; Dong et al., 2020a). Peptide interaction with the receptor junctional domain is required for activation, yet this is less well understood than the interactions with the receptor ECD. Progressive truncation of N-terminal amino acids rapidly decreases agonist efficacy, leading to partial agonists or antagonists, in a receptor-dependent manner (Dong et al., 2020b), emphasizing the importance of understanding the nature of the far N-terminal peptide interactions. Secretin(3-27) has been shown

This work was supported by a grant from National Institutes of Health National Institute of General Medical Sciences [Grant R01-GM132095]. P.M.S. is a Senior Principal Research Fellow of the National Health and Medical Research Council of Australia [ID: 1154434]. D.W. is a Senior Research Fellow of the National Health and Medical Research Council of Australia [ID: 1155302].

P.M.S, A.C., and D.W. are shareholders in Septerna Inc. No author has an actual or perceived conflict of interest with the contents of this article.

dx.doi.org/10.1124/molpharm.122.000502.

ABBREVIATIONS: COS-1, African green monkey kidney; ECD, extracellular domain; E_{max}, maximal system response; GPCR, G protein–coupled receptor; homo-Ser, homoserine; K_A, agonist affinity; KRH, Krebs-Ringers-HEPES; N-terminal, amino-terminal; N terminus, amino terminus; pEC_{50}, negative logarithm of EC_{50}; SecR, secretin receptor; TM7, seventh transmembrane segment; WT, wild-type.

to exhibit no intrinsic ability to stimulate cAMP when used in concentrations as high as 0.1 mM (Dengler et al., 2021).

The secretin receptor (SecR) was the first class B1 (also termed "secretin receptor family") receptor to be cloned (Ishihara et al., 1991). It has important physiologic functions in regulating biliary and pancreatic ductular secretion as well as affecting gastric accommodation and emptying, insulin secretion, thermogenesis in brown adipocytes, fluid balance, and cardiovascular function (Sekar and Chow, 2013; Chey and Chang, 2014). Long-duration, potent secretin-like agonists could therefore play roles in the treatment of disorders of gastric emptying like functional dyspepsia, diabetes, obesity, and congestive heart failure. We recently solved the structure of the secretin-occupied SecR in complex with Gs, demonstrating that it has a high degree of homology with the consensus structures of other recently solved family members (Dong et al., 2020a). Nonetheless, we now understand that the dynamics of the agonist-bound receptor can play critically important roles in the pharmacology of individual peptides and receptors (glucagon-like peptide-1 receptors, adrenomedullin receptors, secretin receptors) (Dong et al., 2020b; Liang et al., 2020; Johnson et al., 2021; Zhang et al., 2021; Cary et al., 2022). For example, molecular dynamics simulations of the secretin-bound SecR structure predicted that the distal secretin N-terminal residues formed prominent interactions with E373 in the seventh transmembrane segment (TM7) of the receptor (Dong et al., 2020a). His^1 was in contact with E373 in 94% of frames compared with fewer than 40% of frames for other receptor residues. E373 was also the dominant contact for secretin residue Ser^2, present in 87% of frames, while contacting other receptor residues in fewer than 60% of frames; however, only the interaction between E373 and Ser^2 was evident in the consensus structure (Dong et al., 2020a).

Based on these observations, we sought to carefully explore structure-activity relationships for peptide residues His^1 and Ser^2 and receptor residue E373 in SecR. This work confirmed critically important interactions for both peptide positions and E373 while providing new insights into the molecular basis of natural peptide activation of SecR that are likely more broadly relevant to class B1 GPCR activation.

Materials and Methods

Materials. Secretin(1-27) (secretin) and the secretin analog used for radioiodination, [Tyr^{10}]secretin(1-27), were synthesized as previously described (Ulrich et al., 1993). Dulbecco's modified Eagle's medium (DMEM) and soybean trypsin inhibitor were from Invitrogen (Carlsbad, CA), and FetalClone II culture medium supplement was from Hyclone Laboratories (Logan, UT). LANCE kits and cAMP-Gs dynamics assay kits for quantitation of cAMP were from PerkinElmer Life Sciences (Boston, MA). All other reagents were analytical grade.

Peptides. Structure-activity relationship studies have shown that the peptide N-terminal region is critical for both binding and receptor signaling (Neumann et al., 2008; Watkins et al., 2012). In the current study, the first two amino acid residues at the N terminus of secretin were each systematically replaced with residues having distinct defined chemical properties. His^1 is a basic amino acid that was replaced with its stereoisomer, *D*-His, as well as with other basic residues, Arg or Lys, charge-reversed acidic Glu, hydrophobic Cha (3-cyclohexyl-*L*-alanine), or polar uncharged homo-Ser (homoserine). Ser^2 is a polar uncharged amino acid that was replaced by its stereoisomer, *D*-Ser, a residue with the same side chain that is extended by one additional carbon residue, homo-Ser, another chemically similar residue, Thr, acidic Glu, basic Lys, or Dap (*L*-2,4-diaminopropionic acid) (Fig. 1). These peptides were synthesized in-house or by Apeptide Company (Shanghai, China) and were purified to greater than 95% purity, with their identities verified by electrospray ionization mass spectrometry.

Receptor Mutagenesis. SecR had the codon for the acidic glutamic acid residue in position 373 replaced with codons for acidic aspartic acid (E373D), uncharged glutamine (E373Q), and basic arginine (E373R) using oligonucleotide-directed mutagenesis of the wild-type construct in pcDNA3 expression vector as we have described (Dong et al., 2012). All constructs were verified by DNA sequencing.

Radioiodination. The secretin-like radioligand [^{125}I-Tyr^{10}] secretin(1-27) was prepared by oxidative radioiodination using established procedures (Powers et al., 1988). In brief, ~15 μg of [Tyr^{10}] secretin(1-27) was incubated with 1 mCi $Na^{125}I$ (PerkinElmer) in 0.1 M borate buffer (pH 9.0) and exposed for 15 seconds to the solid phase oxidant, *N*-chlorobenzene sulfonamide (Iodobeads; Pierce, Rockford, IL). The radioiodinated peptide was purified by reverse-phase high-performance liquid chromatography (HPLC) to yield specific radioactivity of approximately 2000 Ci/mmol.

Cell Culture and Transfection. COS-1 (African green monkey kidney) cells (American Type Culture Collection, Manassas, VA) were used for transient expression of SecR mutant constructs. Cells were grown in tissue culture plasticware using Dulbecco's modified

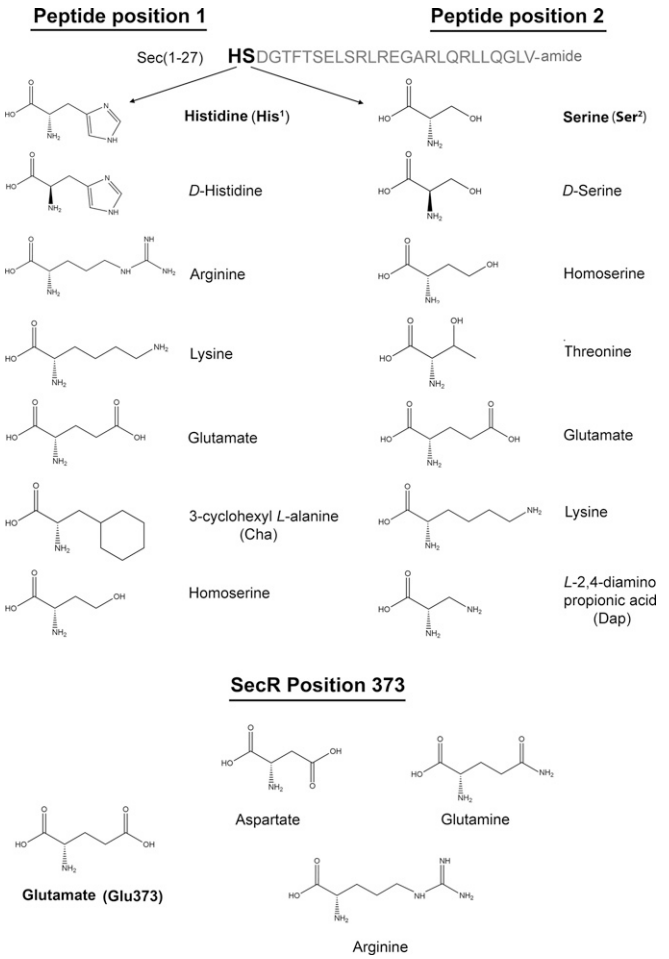

Fig. 1. Structures of natural and unnatural amino acids incorporated into positions one and two of secretin peptides and those used to replace Glu in position 373 of SecR. Shown are the chemical structures of the residues used in peptide structure-activity series. The remaining peptide sequences were identical to natural human secretin(1-27).

Eagle's medium (DMEM) supplemented with 2 mM glutamine and 5% FetalClone II as well as 100 IU/ml penicillin and 100 μg/ml streptomycin, in an environment including 5% CO_2. They were passaged approximately twice per week. Cells were transfected using the diethylaminoethyl (DEAE)-dextran protocol (Hadac et al., 1996) approximately 48 hours prior to assays.

Receptor Binding Assays. Receptor binding characteristics were determined in radioligand competition-binding assays using whole cells expressing the SecR constructs (Dong et al., 2012). Transfected COS-1 cells achieving approximately 90% confluence were washed with Krebs-Ringers-HEPES (KRH) medium (25 mM HEPES, pH 7.4, 104 mM NaCl, 5 mM KCl, 2 mM $CaCl_2$, 1 mM KH_2PO_4, 1.2 mM $MgSO_4$) containing 0.01% soybean trypsin inhibitor and 0.2% bovine serum albumin and were incubated with a constant amount of radioligand [^{125}I-Tyr^{10}]secretin(1-27) (11 pM, approximately 10,000 cpm) and increasing concentrations of secretin or secretin analogs for 60 minutes at room temperature. After incubation, cells were washed twice with ice-cold KRH medium and lysed with 0.5 M NaOH, and membrane-bound radioactivity was quantified with a γ-spectrometer. Nonsaturable binding was determined in the presence of 1 μM secretin, representing less than 17% of total binding. This value was used as B_0, whereas radioligand binding in the absence of competing ligand was used as B_{max} in plotting the amount of saturable binding present in competition-binding curves. These plots were analyzed using the nonlinear regression analysis routine in the Prism 9.0 software suite (GraphPad, San Diego, CA).

cAMP Assays. Cellular cAMP was quantified using LANCE cAMP assay and cAMP-Gs dynamics assay kits (PerkinElmer, Boston, MA) (Harikumar et al., 2007). In short, COS-1 cells expressing SecR constructs were grown in 96-well plates used to examine the ability of each of the secretin analogs to stimulate cAMP responses. Combinations of peptide and receptor constructs that elicited no significant cAMP response were also tested for antagonist activity, utilizing a submaximal concentration of secretin and increasing concentrations of the potential antagonist. Cells were washed once with phosphate-buffered saline (PBS) and incubated with increasing concentrations of secretin or secretin analogs in KRH medium containing 0.1% bacitracin and 1 mM 3-isobutyl-1-methylxanthine for 30 minutes at 37°C. The reaction was stopped by aspiration of the solution, and cells were lysed with 6% ice-cold perchloric acid for 15 minutes with vigorous shaking. After adjusting pH to 6 with 30% $KHCO_3$, cell lysates were assayed for cAMP levels in a 384-well white OptiPlate using the kits, following the manufacturer's instructions. All conditions were assayed in duplicate in a minimum of five independent experiments. Results were read using a PHERAstar FSX (BMG LabTech Inc., Cary, NC) with the homogeneous time-resolved fluorescence protocol.

The cAMP concentration-response curves were plotted using a three-parameter logistic equation in Prism 9.0 (GraphPad) as previously described (May et al., 2007; Koole et al., 2010), fixing the top (maximal stimulation in the presence of ligands) and bottom (Y value in the absence of ligands) to 100 and 0, respectively, for the response to native secretin peptide. Maximal system response (E_{max}) (expressed as a percentage of the secretin response) and pEC_{50} (negative log molar concentration of ligand required to generate a response halfway between top and bottom) were derived for each peptide and receptor construct. Data were also analyzed with an operational model to estimate the ratio of tau (τ), the index of coupling efficiency (or efficacy) defined as the total concentration of agonist-receptor complex that yields half the maximal system response (E_{max}), to the agonist affinity (K_A) as previously described (Koole et al., 2010). This ratio reflects the efficacy of the agonists to stimulate cAMP.

Secretin Receptor Immunostaining. To determine levels of cell surface expression of the SecR mutant constructs, immunostaining was performed using an antibody previously described to target the N-terminal region of SecR (Dong et al., 2020a). Transfected COS-1 cells grown on polylysine-coated glass coverslips in six-well plates were washed with PBS and fixed with 2% paraformaldehyde

TABLE 1

Binding and biologic activity of position 1 secretin analogs at SecR and position 373 mutants. Values are expressed as means ± S.E.M. from duplicate determinations in "n" independent experiments (shown in parentheses). Values were analyzed using one-way ANOVA with Dunnett's post-test compared with secretin effects at respective constructs.

Constructs	Ligands	pK_i	(n), *P* value	pEC_{50}	(n), *P* value	E_{max}	*P* value	Log (τ/K_A ratio)	*P* value
WT	Secretin	8.5 ± 0.2	(5)	10.2 ± 0.3	(5)	97 ± 2		10.2 ± 0.1	
	Sec-*D* His[1]	8.0 ± 0.1	(7), 0.1857	10.1 ± 0.1	(5) 0.9951	97 ± 10	>0.9999	10.1 ± 0.1	0.9730
	Sec-Arg[1]	7.4 ± 0.2**	(5), 0.0012	7.5 ± 0.3***	(5), <0.0001	59 ± 6*	0.0127	6.9 ± 0.2***	<0.0001
	Sec-Lys[1]	7.2 ± 0.1***	(5), <0.0001	7.2 ± 0.3***	(5), <0.0001	54 ± 10**	0.0048	6.6 ± 0.2***	<0.0001
	Sec-Glu[1]	6.2 ± 0.2***	(7), <0.0001	7.4 ± 0.1***	(5), <0.0001	67 ± 9	0.0666	7.0 ± 0.2***	<0.0001
	Sec-Cha[1]	7.9 ± 0.1	(5), 0.0729	8.9 ± 0.3**	(5), 0.0025	79 ± 10	0.4208	8.6 ± 0.2***	<0.0001
	Sec-homo-Ser[1]	7.3 ± 0.3***	(5), 0.0004	7.4 ± 0.2***	(5), <0.0001	47 ± 8***	0.0009	6.7 ± 0.3***	<0.0001
E373D	Secretin	8.4 ± 0.2	(5)	10.1 ± 0.1	(5)	101 ± 4		10.1 ± 0.1	
	Sec-*D* His[1]	8.0 ± 0.2	(7), 0.1060	10.0 ± 0.1	(5), 0.9723	37 ± 8***	<0.0001	9.3 ± 0.2*	0.0285
	Sec-Arg[1]	7.5 ± 0.1***	(6), 0.0001	7.5 ± 0.2***	(5), <0.0001	39 ± 4***	<0.0001	6.7 ± 0.2***	<0.0001
	Sec-Lys[1]	7.3 ± 0.1***	(5), <0.0001	7.1 ± 0.2***	(5), <0.0001	25 ± 2***	<0.0001	6.1 ± 0.3***	<0.0001
	Sec-Glu[1]	6.7 ± 0.1***	(5), <0.0001	7.1 ± 0.2***	(5), <0.0001	50 ± 2***	<0.0001	6.5 ± 0.2***	<0.0001
	Sec-Cha[1]	8.2 ± 0.1	(5), 0.7766	8.7 ± 0.2***	(5), <0.0001	48 ± 5***	<0.0001	8.2 ± 0.2***	<0.0001
	Sec-homo-Ser[1]	7.3 ± 0.1***	(5), <0.0001	7.3 ± 0.1***	(6), <0.0001	48 ± 2***	<0.0001	6.8 ± 0.2***	<0.0001
E373Q	Secretin	8.5 ± 0.1	(5)	9.1 ± 0.2	(7)	102 ± 7		9.2 ± 0.1	
	Sec-*D* His[1]	8.1 ± 0.3	(7), 0.4932	8.6 ± 0.2	(8), 0.1169	77 ± 14	0.1884	8.3 ± 0.2	0.0674
	Sec-Arg[1]	8.1 ± 0.1	(5), 0.5525	NR		NR		NR	
	Sec-Lys[1]	7.8 ± 0.1	(7), 0.1220	NR		NR		NR	
	Sec-Glu[1]	7.0 ± 0.1***	(6), 0.0001	6.8 ± 0.1***	(5), <0.0001	32 ± 4***	0.0004	6.2 ± 0.5***	<0.0001
	Sec-Cha[1]	8.0 ± 0.2	(6), 0.4868	8.3 ± 0.1*	(5), 0.0143	45 ± 7**	0.0030	8.4 ± 0.4	0.1361
	Sec- homo-Ser[1]	7.8 ± 0.4	(5), 0.1746	NR		NR		NR	
E373R	Secretin	8.3 ± 0.3	(7)	8.1 ± 0.1	(5)	78 ± 4		8.0 ± 0.2	
	Sec-*D* His[1]	7.9 ± 0.1	(7), 0.1418	7.3 ± 0.2*	(7), 0.0195	92 ± 18	0.8776	7.5 ± 0.5	0.6516
	Sec-Arg[1]	7.6 ± 0.1**	(6), 0.0087	NR		NR		NR	
	Sec-Lys[1]	7.5 ± 0.1**	(7), 0.0014	NR		NR		NR	
	Sec-Glu[1]	ND		6.8 ± 0.1***	(5), 0.0005	55 ± 22	0.6682	6.7 ± 0.4	0.1010
	Sec-Cha[1]	8.3 ± 0.1	(7), >0.9999	7.6 ± 0.3	(5), 0.1477	56 ± 14	0.7161	7.8 ± 0.4	0.9821
	Sec-homo-Ser[1]	ND		NR		NR		NR	

ND, no detectable binding; NR, no significant biologic response.
*$P < 0.05$; **$P < 0.01$; ***$P < 0.001$.

(Electron Microscopy Sciences, Hatfield, PA). The coverslips were washed twice with PBS containing 1% normal goat serum and incubated overnight at 4°C with the anti-hSecR(51-65) (1:200 in PBS with 1% normal goat serum). They were washed three more times and were incubated for 1 hour at room temperature with Alexa Fluor 488-conjugated anti-rabbit IgG (Molecular Probes, Eugene, OR) diluted 1:800 in PBS with 1% normal goat serum in a humidified chamber. Coverslips were washed three more times with PBS and were mounted on microscope slides with VECTASHIELD mounting medium (Vector Laboratories, Burlingame, CA). Cells were visualized with a 40× objective on a Zeiss inverted microscope controlled by QED InVivo software (Media Cybernetics, Bethesda, MD).

Quantitation of cell surface receptor was performed on a minimum of twenty cells for each construct using Image J (National Institutes of Health, Bethesda, MD).

Statistical Analysis. Comparisons of experimental groups were assessed using one-way analysis of variance (ANOVA) followed by Dunnett's post-test as provided in Prism 9.0 (GraphPad, San Diego, CA). This was typically used to determine the differences of binding and biologic activity of secretin analog peptides relative to that of natural secretin at a particular secretin receptor construct. The threshold for statistical significance was set at $P < 0.05$; P values are shown in Tables 1 and 2.

Results

Structure-Activity Relationships for Secretin Residues His^1 and Ser^2. The natural amino acids in secretin peptide positions one and two were systematically modified with other natural or unnatural amino acids having distinct chemical properties as detailed in Fig. 1. All of the peptides competed for binding of [^{125}I-Tyr^{10}]secretin(1-27) to wild-type SecR, although reductions in binding affinities were statistically significant in many cases (Fig. 2; Tables 1 and 2). Similarly, all peptides stimulated cAMP accumulation at wild-type SecR, although with varied potencies and maximal responses (Fig. 3; Tables 1 and 2). We also show the τ/K_A ratios coming from the operational model as a reflection of efficacy of the ligands (Tables 1 and 2).

For the position 1 peptides, His^1 replacement by its stereoisomer, *D*-His, or hydrophobic Cha had no effect on binding affinity, whereas the other substitutions displayed reduced affinity (Fig. 2; Table 1). Thus, the charge of His^1 is not critical for binding affinity, whereas substitution for the extended Arg or Lys residues was detrimental to affinity. Only the *D*-His peptide elicited an equivalent cAMP response to the natural peptide; all other substitutions reduced signaling by at least 10-fold (Fig. 3; Table 1). It was notable that Arg/Lys substitutions induced greater reductions in efficacy (2000- and 4000-fold, respectively) than on binding affinity (13- and 20-fold, respectively) (Table 1). However, changing the orientation of the His (*D*-His) did not alter binding or signaling, indicating that it retained sufficient mobility within the receptor to form critical interactions.

For the position 2 peptides, every replacement of Ser^2, including *D*-Ser, reduced binding affinity (Fig. 2; Table 2), indicating a precise structural requirement for optimal interaction that does not accommodate even small changes to the

TABLE 2
Binding and biologic activity of position 2 secretin analogs at SecR and position 373 mutants. Values are expressed as means ± S.E.M. from duplicate determinations in "n" independent experiments (shown in parentheses). Values were analyzed using one-way ANOVA with Dunnett's post-test compared with secretin effects at respective constructs.

Constructs	Ligands	pK_i	(n), P value	pEC_{50}	(n), P value	E_{max}	P value	Log (τ/K_A ratio)	P value
WT	Secretin	8.5 ± 0.2	(5)	10.2 ± 0.3	(5)	97 ± 2		10.1 ± 0.1	
	Sec-*D* Ser^2	7.2 ± 0.1**	(5), 0.0060	9.0 ± 0.1***	(5), 0.0003	81 ± 12	0.7788	8.9 ± 0.2***	<0.0001
	Sec-homo-Ser^2	7.3 ± 0.2*	(5), 0.0167	8.9 ± 0.1***	(5), 0.0001	80 ± 10	0.7316	8.7 ± 0.2***	<0.0001
	Sec-Thr^2	7.5 ± 0.05*	(5), 0.0371	9.4 ± 0.1*	(6), 0.0121	111 ± 14	0.8484	9.4 ± 0.1**	0.0098
	Sec-Glu^2	7.2 ± 0.5**	(5), 0.0051	7.4 ± 0.1***	(5), <0.0001	93 ± 11	0.9995	7.2 ± 0.2***	<0.0001
	Sec-Lys^2	6.8 ± 0.1***	(5), 0.0003	7.9 ± 0.2***	(5), <0.0001	68 ± 8	0.2215	7.4 ± 0.2***	<0.0001
	Sec-Dap^2	7.5 ± 0.3*	(5), 0.0352	9.0 ± 0.1***	(5), 0.0004	88 ± 8	0.9751	8.9 ± 0.2***	<0.0001
E373D	Secretin	8.4 ± 0.2	(5)	10.1 ± 0.1	(5)	101 ± 4		10.1 ± 0.1	
	Sec-*D* Ser^2	7.3 ± 0.1***	(5), <0.0001	8.9 ± 0.1***	(6), <0.0001	69 ± 8	0.1680	8.8 ± 0.2***	0.0001
	Sec-homo-Ser^2	7.3 ± 0.1***	(5), 0.0001	9.2 ± 0.1***	(7), <0.0001	62 ± 8*	0.0485	8.9 ± 0.2***	0.0005
	Sec-Thr^2	7.4 ± 0.1***	(5), 0.0003	9.2 ± 0.1***	(7), <0.0001	86 ± 11	0.8088	9.1 ± 0.1**	0.0033
	Sec-Glu^2	6.7 ± 0.1***	(6), <0.0001	7.6 ± 0.1***	(5), <0.0001	68 ± 18	0.1756	7.3 ± 0.2***	<0.0001
	Sec-Lys^2	6.9 ± 0.2***	(5), <0.0001	7.9 ± 0.1***	(5), <0.0001	51 ± 9*	0.0136	7.5 ± 0.3***	<0.0001
	Sec-Dap^2	7.3 ± 0.2***	(5), 0.0001	8.7 ± 0.2***	(6), <0.0001	74 ± 8	0.3062	8.5 ± 0.2***	<0.0001
E373Q	Secretin	8.5 ± 0.1	(5)	9.1 ± 0.2	(7)	102 ± 7		9.2 ± 0.1	
	Sec-*D* Ser^2	7.6 ± 0.1*	(5), 0.0147	7.7 ± 0.1***	(5), <0.0001	114 ± 30	0.9933	7.8 ± 0.2***	<0.0001
	Sec-homo-Ser^2	7.4 ± 0.1**	(5), 0.0021	7.9 ± 0.1***	(5), 0.0007	66 ± 11	0.5879	7.9 ± 0.2***	0.0003
	Sec-Thr^2	7.7 ± 0.1*	(7), 0.0194	8.0 ± 0.2***	(5), 0.0009	76 ± 10	0.8387	8.0 ± 0.2**	0.0012
	Sec-Glu^2	7.6 ± 0.2**	(5), 0.0094	8.1 ± 0.1**	(8), 0.0012	93 ± 9	0.9979	8.1 ± 0.1***	0.0004
	Sec-Lys^2	7.2 ± 0.1***	(5), 0.0001	<6	—	—			
	Sec-Dap^2	7.9 ± 0.4	(5), 0.1877	7.4 ± 0.1***	(10), <0.0001	93 ± 23	0.9980	7.6 ± 0.2***	<0.0001
E373R	Secretin	8.3 ± 0.3	(7)	8.1 ± 0.1	(5)	78 ± 4		8.3 ± 1.5	
	Sec-*D*-Ser^2	7.5 ± 0.2**	(5), 0.0059	<6					
	Sec-homo-Ser^2	ND		NR		NR		NR	
	Sec-Thr^2	7.5 ± 0.1**	(6), 0.0068	7.7 ± 0.2	(5), 0.7741	105 ± 23	0.6735	8.0 ± 1.8	0.9995
	Sec-Glu^2	7.5 ± 0.1**	(7), 0.0036	7.3 ± 0.6	(8), 0.4160	162 ± 17**	0.0026	8.0 ± 0.2	0.9980
	Sec-Lys^2	7.5 ± 0.1**	(6), 0.0037	NR		NR		NR	
	Sec-Dap^2	ND		NR		NR		NR	

ND, no detectable binding; NR, no significant biologic response.
*$P < 0.05$; **$P < 0.01$; ***$P < 0.001$.

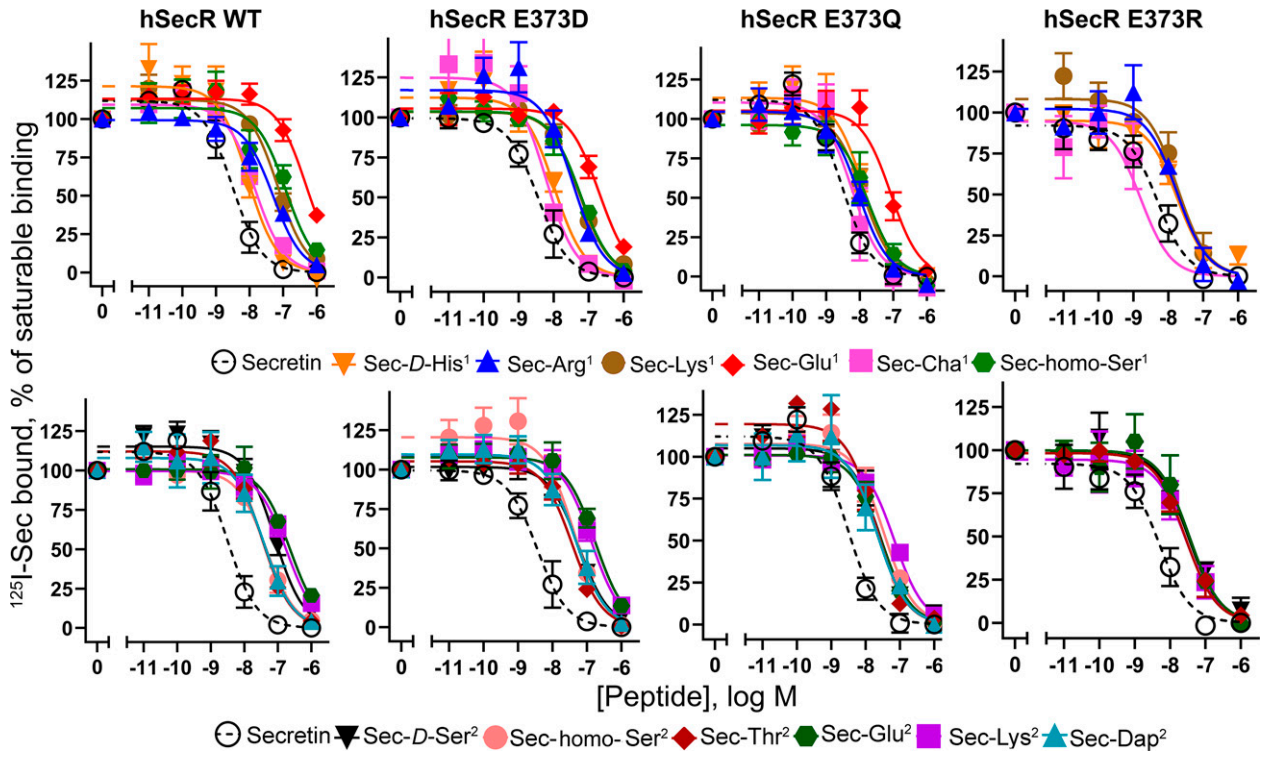

Fig. 2. Binding of secretin and its analogs at SecR and its position 373 mutants. Shown are peptide competition-binding curves at wild-type SecR and its E373D, E373Q, and E373R mutant constructs. Data reflect means ± S.E.M. of assays performed in duplicate in five to seven independent experiments.

side chain, including a single carbon atom extension (homo-Ser) and chemically similar Thr (Fig. 1). Changing the orientation of the Ser in position 2 was detrimental, reducing the binding affinity and signaling of this peptide. However, the quantitative impact on affinity and potency were similar for position 2–substituted peptides at wild-type SecR, indicating that the effects were largely driven by the reduction in binding affinity.

Structure-Activity Relationships for Secretin Receptor E373. E373 is predicted to form the dominant contact for both His^1 and Ser^2 in equilibrium molecular dynamics (Dong et al., 2020a). Glutamic acid is both polar and acidic with an extended alkyl chain that can provide additional hydrophobic interactions. Electrostatic interactions between opposing charged residues are energetically favorable and can occur over longer atomic distances than polar H-bonds. Here, we explored the nature of the chemical interaction with the peptides through mutation of the glutamic acid to residues that modified the side chain length (E373D), charge but not polarity (E373Q), or reversed the charge (E373R) (structures shown in Fig. 1). All of these position 373 mutant receptors trafficked normally to the cell surface, as demonstrated by immunostaining of intact cells that showed that all of these constructs were expressed at similar levels (Fig. 4). Each of these position 373 mutants exhibited secretin binding affinity and functional responses like that at wild-type (WT) SecR (Figs. 2 and 3; Tables 1 and 2). The effect of the Sec-Glu^2 peptide at the charge-reversed E373R construct was notable since it elicited a greater cAMP response than natural secretin. This was not simply due to introduction of a charge-charge interaction since reversing these charges (Sec-Lys^2 peptide at WT SecR or E373D mutant) did not elicit a similar effect. The position of the charge on glutamic acid and/or the extended chain of the glutamic acid allowing hydrophobic interactions not possible with aspartic acid may have also contributed to this unusual effect.

Effect of E373 mutation on peptide analog binding affinity. Overall, mutation of E373 to Asp or Gln had minimal effect on the relative affinity of either position 1– or position 2–substituted peptides compared with their effects at wild-type SecR, although there was a trend for the Arg^1 or Lys^1 substitutions to be less impacted at the E373Q mutant (Fig. 2; Table 1).

Effect of E373 mutation on peptide analog cAMP response. Mutation of E373 to the shorter acidic residue Asp globally reduced the maximal response of position 1–substituted analogs relative to the native secretin peptide (Fig. 3; Table 1), suggesting that this natural glutamic acid may have an important role beyond its charge alone. This could reflect optimal positioning for a transient or stable interaction with the serine in position 2 of secretin or in an intramolecular interaction that could contribute to receptor activation. However, overall, the potencies of peptide 1 analogs were like those seen for the wild-type SecR (Fig. 3; Table 1). In contrast, there was less impact of the mutation on E_{max} for position 2–substituted analogs, although there were greater losses in potency for the Thr^2 analog relative to the wild-type receptor (Fig. 3; Table 2).

Mutation of E373 to the noncharged polar equivalent (Gln) provided further important insights into the interaction requirements for cAMP signaling. Intriguingly, there were no demonstrable cAMP responses to Lys^1 or Arg^1 analogs. This was also true for homo-Ser^1, whereas the Cha^1 analog exhibited reduced maximal responses. The *D*-His^1 analog

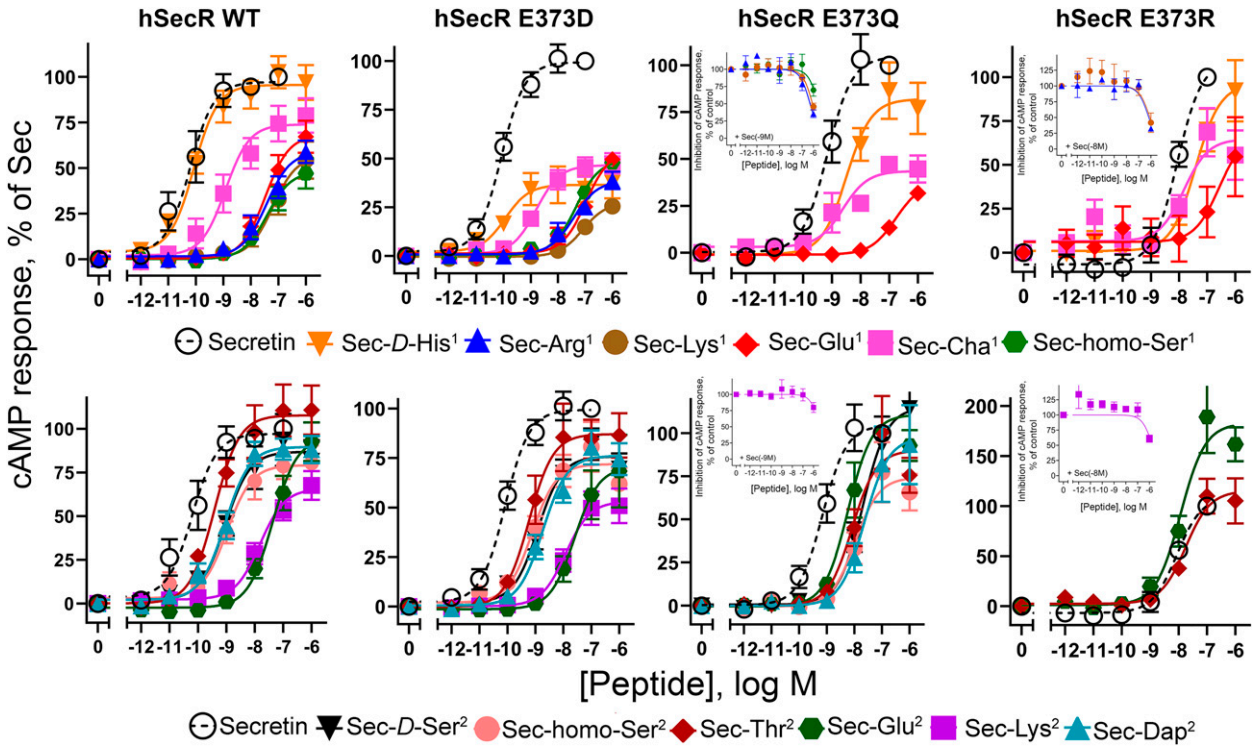

Fig. 3. Biologic activity of secretin and its analogs at SecR and its position 373 mutants. Shown are peptide concentration-response curves at wild-type SecR and its E373D, E373Q, and E373R mutant constructs. Data reflect means ± S.E.M. of assays performed in duplicate in five to eight independent experiments. Inset data represent concentration-response curves for noted peptides that had no significant intrinsic agonist activity at the E373Q and E373R constructs to inhibit cAMP responses to 1 or 10 nM secretin, representing approximate EC_{50}s.

exhibited responses similar to natural secretin at this construct. The position 2 peptide analogs were generally less affected by the E373Q mutant. All except the Dap^2 peptide bound with reduced affinity relative to the natural secretin peptide (Fig. 2; Table 2), with corresponding loss or relative potency in cAMP assay. An exception to this was the Lys^2 peptide that elicited only minimal response (Fig. 3; Table 2).

Mutation of E373 to Arg (E373R), reversing its charge, had dramatically different effects on cAMP signaling of the peptide analogs. Several peptides did not stimulate cAMP even at the highest concentration assessed. These included Arg^1, Lys^1, homo-Ser^1, homo-Ser^2, Lys^2, and Dap^2. Of note, the Glu^2 peptide elicited an increased cAMP response above natural secretin at the E373R construct. Those peptides that were able to bind but not elicit a cAMP response were tested for possible antagonist activity by incubating them with an approximate EC_{50} concentration of secretin. Insets in relevant graphs in Fig. 3 illustrate their abilities to inhibit the secretin-stimulated cAMP responses (E373Q construct: Arg^1, 6.4 ± 0.1; Lys^1, 6.1 ± 0.1; homo-Ser^1, 5.7 ± 0.1; Lys^2, 5.6 ± 0.1, $n = 3$, $P < 0.05$; E373R construct: Arg^1, 6.2 ± 0.1; Lys^1, 6.1 ± 0.3; Lys^2, 5.7 ± 0.1, $n = 3$ to 4, $P < 0.05$).

Discussion

The N-terminal residues of natural peptide ligands of class B1 GPCRs are critically important for their ability to stimulate a cAMP response (Miller et al., 2012; Watkins et al., 2012). Truncation of these residues often markedly reduces or totally eliminates their functional responses while retaining high binding affinity that is principally driven by interaction of the peptide carboxyl-terminal (C-terminal) segments with the receptor ECD (Dong et al., 2020b). However, the specific molecular interactions that are crucial for this agonist activity are not well understood, even where the N-terminal residues are highly conserved between peptides (Neumann et al., 2008; Watkins et al., 2012). Moreover, recent analysis of class B GPCR structures has revealed that dynamics of the interactions between the peptide N terminus and the receptor core can be highly dynamic (Dong et al., 2020a; Cary et al., 2022).

In this work, we focus on the first two amino acid residues at the N terminus of secretin, His^1 and Ser^2, which are critical for the agonist activity of this peptide (Dengler et al., 2021). We explored the critical chemical features of the side-chains of these residues, both in the context of wild-type SecR and in mutant receptors where the length and charge of the principal receptor contact for these residues are modified. We also focused on a key residue in the junctional domain of SecR, Glu373, that interacted with these ligand residues in our previously reported cryo-electron microscopy (cryo-EM) structure and/or molecular dynamics simulations (Dong et al., 2020a). The approximation of this portion of the peptide and the receptor is shown in Fig. 5.

A potential mechanism for peptide engagement with the deeper core of the transmembrane domain that is seen in high-resolution consensus structures is for charge-charge interactions with basic His^1 to orient the N terminus during binding transitions from initial interactions. Our data demonstrate that this is not critical for binding per se since basic His^1 could be replaced by uncharged Cha without reducing affinity. Nonetheless, this form of the peptide was less potent than natural secretin in activating the receptor, suggesting

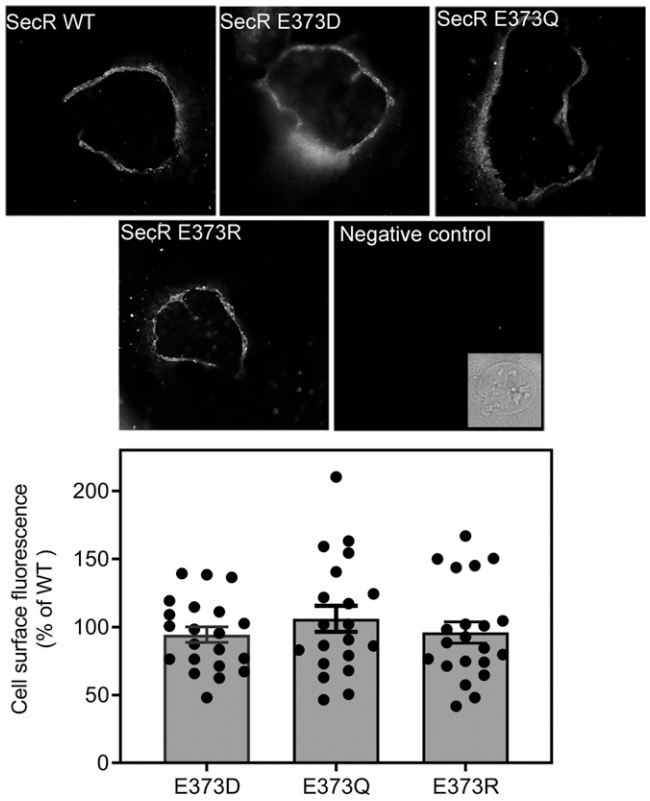

Fig. 4. Cell surface expression of position 373 SecR mutants. Shown are representative immunostained COS-1 cells transfected with noted SecR constructs and quantitation of surface expression of these constructs using densitometry. Shown are individual values and S.E.M. of their variation. Levels of cell surface expression were not different in any of these mutants from wild-type SecR.

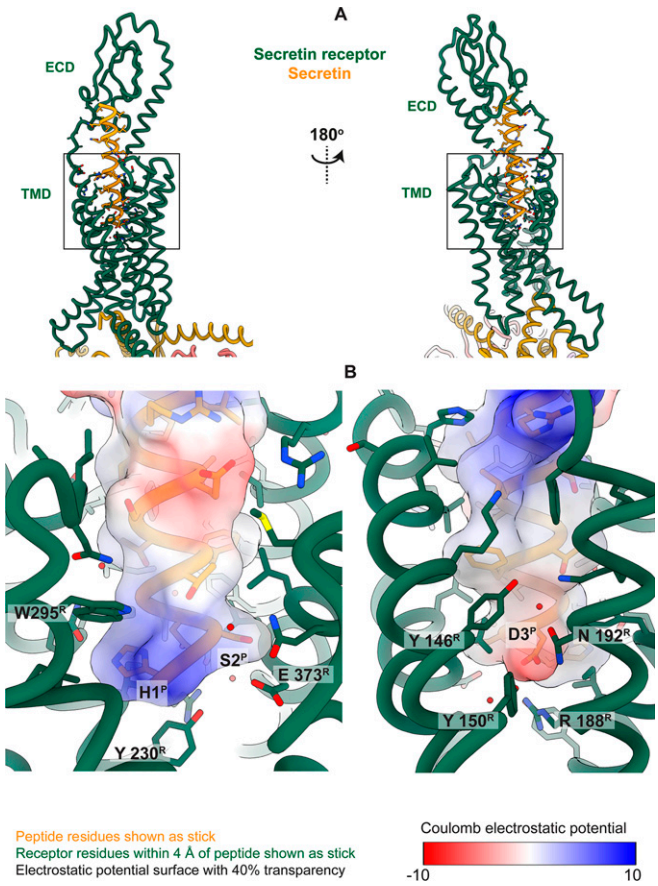

Fig. 5. Characteristics of junctional domain surface of secretin receptor. Shown is an overview of the deep binding pocket from our secretin/SecR complex structure (PDB 6wzg) (Dong et al., 2020a) but with waters added to the surface of the junctional domain of SecR, as solved in our recent publication (Dong et al., 2020a) (A, top panels with front and back views shown). The lower panels (B) show expanded views of the transmembrane domain (TMD) regions blocked above, with the coulomb electrostatic surface coloring of the peptide. Peptide residues are shown as stick, and receptor residues within 4 Å of the peptide are also shown as stick.

that a charge-charge interaction might facilitate the conformational change necessary to mediate activation. Interestingly, *D*-His was able to replace *L*-His in position 1 without any negative impact on binding or receptor signaling, indicating that there is a degree of conformational flexibility within the binding pocket. However, here too, other basic residues like Arg or Lys were poor replacements for His[1]. The functional importance of a charge-charge interaction was also supported by mutation of the predicted receptor target for this interaction, the acidic Glu373 in transmembrane 7 of the secretin receptor. This residue could not be replaced with the shorter acidic Asp (E373D) without reducing the efficacy of all of the position 1 peptides except natural secretin and reducing the potency of all of these peptides except the *D*-His[1] peptide. Nonetheless, the Cha[1] peptide was the least affected of the other analogs. Eliminating the charge of Glu373 through mutation to Gln (E373Q) resulted in elimination of cAMP responses to the Arg[1], Lys[1], and homo-Ser[1] peptides. Collectively, these data demonstrate a role for both the charge and aromatic properties of His[1] in productive activation of the SecR and support the importance of the predicted interaction with Glu373 in activation of the receptor.

Glu373 is also postulated to interact with Ser[2] of the secretin peptide, forming polar interactions in our molecular dynamics analysis (Dong et al., 2020a). Almost every change in the position 2 residue resulted in reduced binding affinity to wild-type secretin receptor as well as to the E373D and E373Q receptor constructs. This even includes residues with similar chemical properties (Thr) and the same functional group spaced one carbon further from the backbone (homo-Ser) or presented as a stereoisomer (*D*-Ser). Of particular interest, some of the position 2 peptides that lost considerable binding affinity still supported potent biologic responses at wild-type secretin receptor. These data indicate that secretin binding is dependent on the efficiency of H-bond formation between the receptor and Ser[2] but that this is not independently required for receptor activation.

The E373 mutation data, however, suggests that enabling longer distance charge-charge interactions can at least partially overcome the conformational requirements to support H-bonding to Ser[2] in the native peptide. This is evidenced by the acidic Glu[2] peptide substitution. This analog was much less potent than natural secretin [log (τ/K_A ratio)] at wild-type secretin receptor (7.2 ± 0.2 vs. 10.1 ± 0.1, representing an 800-fold reduction, $P < 0.001$) and at the similarly charged E373D construct (7.3 ± 0.2 vs. 10.1 ± 0.1, representing a 600-fold reduction, $P < 0.001$) yet was equipotent with natural secretin at the charge-reversed E373R construct (8.0 ± 0.2 vs. 8.3 ± 1.5, $P = 1.00$). Additionally, the peptide including a basic Lys residue in position 2 was active at SecR having acidic

Glu in position 373 [log (τ/K_A ratio)], 7.4 ± 0.2) and at E373D (7.5 ± 0.3) while exhibiting minimal or no activity at those receptors in which an acidic residue is absent in this position (E373Q (minimal detectable agonist activity) and E373R (no detectable agonist activity). In the active structure of secretin bound SecR, Ser^2 and E373 are proximal to each other, suggesting that interaction between these residues helps the coordination of the peptide in the deep pocket that is required for receptor activation.

The insights from this systematic analysis of key interacting residues in the natural full agonist secretin peptide and its receptor should help direct future drug development at this important receptor. The success with complementary modification of peptide and receptor, often quite challenging for flexible peptide ligands, further supports understanding of possible forces and movements associated with receptor activation for this and other class B GPCRs.

Authorship Contributions

Participated in research design: Wootten, Sexton, Miller.

Conducted experiments: Milburn, Harikumar, Raval.

Performed data analysis: Milburn, Harikumar, Piper, Raval, Wootten, Sexton, Miller.

Wrote or contributed to the writing of the manuscript: Harikumar, Piper, Christopoulos, Wootten, Sexton, Miller.

References

Cary BP, Deganutti G, Zhao P, Truong TT, Piper SJ, Liu X, Belousoff MJ, Danev R, Sexton PM, Wootten D, et al. (2022) Structural and functional diversity among agonist-bound states of the GLP-1 receptor. *Nat Chem Biol* **18**:256–263.

Castro M, Nikolaev VO, Palm D, Lohse MJ, and Vilardaga JP (2005) Turn-on switch in parathyroid hormone receptor by a two-step parathyroid hormone binding mechanism. *Proc Natl Acad Sci USA* **102**:16084–16089.

Chey WY and Chang TM (2014) Secretin: historical perspective and current status. *Pancreas* **43**:162–182.

de Graaf C, Donnelly D, Wootten D, Lau J, Sexton PM, Miller LJ, Ahn JM, Liao J, Fletcher MM, Yang D, et al. (2016) Glucagon-like peptide-1 and its class B G protein-coupled receptors: a long march to therapeutic successes. *Pharmacol Rev* **68**: 954–1013.

de Graaf C, Song G, Cao C, Zhao Q, Wang MW, Wu B, and Stevens RC (2017) Extending the structural view of class B GPCRs. *Trends Biochem Sci* **42**:946–960.

Dengler DG, Harikumar KG, Pollari S, Sun Q, Brown BT, Shinoki-Iwaya A, Ardecky R, Miller LJ, and Sergienko EA (2021) Discovery of small molecule positive allosteric modulators of the secretin receptor. *Biochem Pharmacol* **185**:114451.

Dong M, Deganutti G, Piper SJ, Liang YL, Khoshouei M, Belousoff MJ, Harikumar KG, Reynolds CA, Glukhova A, Furness SGB, et al. (2020a) Structure and dynamics of the active Gs-coupled human secretin receptor. *Nat Commun* **11**:4137.

Dong M, Harikumar KG, Raval SR, Milburn JE, Clark C, Alcala-Torano R, Mobarec JC, Reynolds CA, Ghirlanda G, Christopoulos A, et al. (2020b) Rational development of a high-affinity secretin receptor antagonist. *Biochem Pharmacol* **177**: 113929.

Dong M, Xu X, Ball AM, Makhoul JA, Lam PC, Pinon DI, Orry A, Sexton PM, Abagyan R, and Miller LJ (2012) Mapping spatial approximations between the amino terminus of secretin and each of the extracellular loops of its receptor using cysteine trapping. *FASEB J* **26**:5092–5105.

Grace CR, Perrin MH, DiGruccio MR, Miller CL, Rivier JE, Vale WW, and Riek R (2004) NMR structure and peptide hormone binding site of the first extracellular domain of a type B1 G protein-coupled receptor. *Proc Natl Acad Sci USA* **101**: 12836–12841.

Grace CR, Perrin MH, Gulyas J, Digruccio MR, Cantle JP, Rivier JE, Vale WW, and Riek R (2007) Structure of the N-terminal domain of a type B1 G protein-coupled receptor in complex with a peptide ligand. *Proc Natl Acad Sci USA* **104**:4858–4863.

Hadac EM, Ghanekar DV, Holicky EL, Pinon DI, Dougherty RW, and Miller LJ (1996) Relationship between native and recombinant cholecystokinin receptors: role of differential glycosylation. *Pancreas* **13**:130–139.

Harikumar KG, Pinon DI, and Miller LJ (2007) Transmembrane segment IV contributes a functionally important interface for oligomerization of the class II G protein-coupled secretin receptor. *J Biol Chem* **282**:30363–30372.

Hoare SR (2005) Mechanisms of peptide and nonpeptide ligand binding to class B G-protein-coupled receptors. *Drug Discov Today* **10**:417–427.

Hollenstein K, de Graaf C, Bortolato A, Wang MW, Marshall FH, and Stevens RC (2014) Insights into the structure of class B GPCRs. *Trends Pharmacol Sci* **35**: 12–22.

Ishihara T, Nakamura S, Kaziro Y, Takahashi T, Takahashi K, and Nagata S (1991) Molecular cloning and expression of a cDNA encoding the secretin receptor. *EMBO J* **10**:1635–1641.

Johnson RM, Zhang X, Piper SJ, Nettleton TJ, Vandekolk TH, Langmead CJ, Danev R, Sexton PM, and Wootten D (2021) Cryo-EM structure of the dual incretin receptor agonist, peptide-19, in complex with the glucagon-like peptide-1 receptor. *Biochem Biophys Res Commun* **578**:84–90.

Koole C, Wootten D, Simms J, Valant C, Sridhar R, Woodman OL, Miller LJ, Summers RJ, Christopoulos A, and Sexton PM (2010) Allosteric ligands of the glucagon-like peptide 1 receptor (GLP-1R) differentially modulate endogenous and exogenous peptide responses in a pathway-selective manner: implications for drug screening. *Mol Pharmacol* **78**:456–465.

Liang YL, Belousoff MJ, Fletcher MM, Zhang X, Khoshouei M, Deganutti G, Koole C, Furness SGB, Miller LJ, Hay DL, et al. (2020) Structure and dynamics of adrenomedullin receptors AM_1 and AM_2 reveal key mechanisms in the control of receptor phenotype by receptor activity-modifying proteins. *ACS Pharmacol Transl Sci* **3**:263–284.

May LT, Avlani VA, Langmead CJ, Herdon HJ, Wood MD, Sexton PM, and Christopoulos A (2007) Structure-function studies of allosteric agonism at M2 muscarinic acetylcholine receptors. *Mol Pharmacol* **72**:463–476.

Miller LJ, Dong M, and Harikumar KG (2012) Ligand binding and activation of the secretin receptor, a prototypic family B G protein-coupled receptor. *Br J Pharmacol* **166**:18–26.

Neumann JM, Couvineau A, Murail S, Lacapère JJ, Jamin N, and Laburthe M (2008) Class-B GPCR activation: is ligand helix-capping the key? *Trends Biochem Sci* **33**:314–319.

Parthier C, Reedtz-Runge S, Rudolph R, and Stubbs MT (2009) Passing the baton in class B GPCRs: peptide hormone activation via helix induction? *Trends Biochem Sci* **34**:303–310.

Powers SP, Pinon DI, and Miller LJ (1988) Use of N,O-bis-Fmoc-D-Tyr-ONSu for introduction of an oxidative iodination site into cholecystokinin family peptides. *Int J Pept Protein Res* **31**:429–434.

Schwartz TW and Frimurer TM (2017) Structural biology: full monty of family B GPCRs. *Nat Chem Biol* **13**:819–821.

Sekar R and Chow BK (2013) Metabolic effects of secretin. *Gen Comp Endocrinol* **181**:18–24.

Ulrich 2nd CD, Pinon DI, Hadac EM, Holicky EL, Chang-Miller A, Gates LK, and Miller LJ (1993) Intrinsic photoaffinity labeling of native and recombinant rat pancreatic secretin receptors. *Gastroenterology* **105**:1534–1543.

Watkins HA, Au M, and Hay DL (2012) The structure of secretin family GPCR peptide ligands: implications for receptor pharmacology and drug development. *Drug Discov Today* **17**:1006–1014.

Zhang X, Belousoff MJ, Liang YL, Danev R, Sexton PM, and Wootten D (2021) Structure and dynamics of semaglutide- and taspoglutide-bound GLP-1R-Gs complexes. *Cell Rep* **36**:109374.

Address correspondence to: Dr. Laurence J. Miller, Mayo Clinic, 13400 East Shea Boulevard., Scottsdale, AZ 85259. E-mail: miller@mayo.edu; or Dr. Patrick M. Sexton, Monash Institute of Pharmaceutical Sciences, Monash University, 381 Royal Parade, Parkville, VIC 3052, Australia. E-mail: patrick.sexton@monash.edu